A Primary and Backup Protection Algorithm based on Voltage and Current Measurements for HVDC Grids

Mudar Abedrabbo and Dirk Van Hertem
ELECTA/Energyville, Department of Electrical Engineering (ESAT), University of Leuven (KU Leuven)

***Abstract*—DC grids are susceptible to DC side faults, which lead to a rapid rise of the DC side currents. DC side faults should be detected in a very short time before fault currents cause damage to the system or equipment, e.g., exceed the maximum interruptible limits of DC circuit breaker. This paper presents a primary and backup protective data-based algorithm. The proposed algorithm depends on the local voltage and current measurements to detect and identify various kinds of faults in the HVDC grid, both in the forward and backward directions. Linear Discriminant analysis (LDA) is used to derive the thresholds and the operational time frames of the primary and backup protection zones of the algorithm. A sensitivity analysis is performed to investigate the influence of the line inductor value on the decision thresholds and on the operational time frame of the algorithm. Furthermore, two statistical approaches utilizing LDA and quadratic discriminant analysis (QDA) methods are proposed to extend the operational time frame of the algorithm.**

***Index Terms*— HVDC grid, primary protection, backup protection, DCCB.**

I. Introduction

The indispensable transportation of bulk power over long distances and the rapid growth of remote offshore wind farms push toward the wide deployment of HVDC technology. Multi-terminal HVDC (MTDC) system offers attractive features, such as redundancy, flexibility and high reliability of power transfer [1]. The reliability of the HVDC system guarantees the safe and continuous operation of the grid by preventing any failure of the grid components during severe conditions, which can be achieved by a robust protection system [2]. However, the rapid increase of DC fault currents is considered as the main challenge for the HVDC protection system. The protection system should detect, identify and isolate the fault during the first milliseconds of the fault period before the fault currents rise to destructive values and damage the HVDC converter components or the voltage in the entire DC grid drops to unacceptably low values. The protection requirements for DC grids are at least one order of magnitude faster than those in AC systems [3]. Hence, fast detection by protective relays and fast interruption by DC circuit breakers (DCCB) are essential requirements of the HVDC protection system.

The selective HVDC protection system splits the grid into protection zones. Consequently, in case of DC fault, only the DCCBs related to that zone should operate and clear the faulty element to suppress the propagation of the fault to other grid zones [4]. Thus, primary protection should respond to faults in its zone before backup protection is activated. However, backup protection must be capable to detect any abnormal condition and to react accordingly after the failure of the primary protection [5].

Several non-unit protection schemes for MTDC have been proposed in the literature. Current magnitude and its derivative, which is supplied from the DC capacitors of two-level converters, were the followed approach in [6] and [7]. However, in MTDC with modular multi-level converters (MMC), DC side capacitors are not required, and the discharge of the MMC capacitors can be stopped by blocking the arms submodules. Moreover, the derivative of the current is limited by the line inductors. In [8] and [9], voltage-based protection algorithms have been proposed; however, extensive time-domain simulations are necessary to identify the thresholds for small-scale system [5]. A protection algorithm based on voltage magnitude and its derivative to detect and discriminate faults has been proposed in [5]. Nevertheless, its accuracy decreases by reducing the sampling frequency.

This paper presents a non-unit data-based algorithm based on voltage and current measurements to provide primary and backup protection for HVDC grids. The proposed algorithm collects the current and voltage samples and classifies these data to detect, identify and distinguish forward and backward faults. The algorithm exploits the existence of the line inductor and the sign of di/dt to distinguish between the zones. This algorithm provides fast primary protection in case of forward faults in its primary protection zone, and short delay time for backup protective action in case of backward faults. Moreover, it is suitable for any HVDC grid topology which utilizes fast DCCBs and selective protection system.

Within this paper, the principle of operation of the proposed algorithm is described in Section II. A case study is presented in Section III to derive the zones boundaries of the algorithm and to describe the approaches which can be used to extend its time frame. Section IV presents the conclusion.

II. Protection Algorithm

Fig. 1 illustrates the layout of the bus and the protection zones. Each bus connects two or more lines with a relay and circuit breaker at each line terminal. The protection zone 'First Zone' of a relay is bounded by the inductors of the line, while 'Second Zone' covers the first zone and the surrounding cables as shown in Fig. 1. Therefore, any protection algorithm should discriminate between the first zone and second zone [5].

Faults can be described by a rapid drop in voltage and an increase in current. Propagation of voltage drop as well as rate of rise of the current in the grid are retarded due to the existence of the inductors at the terminals of the faulty line which reflect the voltage wave. Furthermore, di/dt can be an indicator of the direction of the fault (forward or backward fault).

The protection algorithm uses the voltages and currents measured at the relay to detect, identify and discriminate faults in the first zone by comparing the measured quantities (instantaneous voltage and current) by a predefined values of voltage and current, and accordingly it generates a tripping signal to the circuit breaker. The voltage and current samples are projected onto a two dimensional plane (UI-plane), where its x-axis is the current and the y-axis is the voltage. The predefined (threshold) values divide the UI-plane into two zones; the first zone where the relay should operate, and the second zone where the relay sees the fault, but only operates in the case it should provide a backup protection. The adjacent relays of each bus exchange two types of signals (S_P and S_b) as shown in Fig. 1, and (1) describes their values.

$$\begin{aligned} &S_P=1,\ S_b=0 && \textit{for Primary Protection Operation}\\ &S_P=0,\ S_b=1 && \textit{for Backup Protection Operation}\\ &S_P=0,\ S_b=0 && \textit{Otherwise} \end{aligned} \quad (1)$$

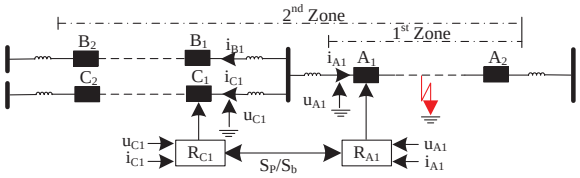

Fig. 1 The general layout of HVDC bus with the protection zones.

A. Principle

The proposed protection algorithm detects faults in the first zone by dividing the UI-plane into two regions, i.e., 'Zone 1' and 'Zone 2'. The boundary of the regions depends on the voltage and current measurements.

The relays R_{B2} and R_{C2} in Fig. 1 see any fault in the 1st zone of R_{A1} as a forward fault; however, the voltage profile and the current magnitudes differ from the measurements at R_{A1} due to the existence of the line inductors. To introduce an independent comparison from the distance between R_{B2} or R_{C2} and R_{A1}, the measurements at R_{B1} and R_{C1} can be considered for the comparison to derive the zones boundaries.

Fig.2 shows the loci of 'u^k' and '$-i^k$' samples at the relays R_{B1} and R_{C1} in Fig. 1 when a fault occurs in the first zone of relay R_{A1}, where u^k is the voltage and $-i^k$ is the negative value of the current. The negative sign is added to the current, since current notation in relay R_{B1} and R_{C1} (i_{B1} and i_{C1}) is in the opposite direction of i_{B2} and i_{C2}. The direction of the arrows illustrates the change of voltage and current as function of time. Fig. 3 describes the continua of the proposed algorithm for primary and backup protection. In Fig. 3, similar to Fig. 2, t_0, $t_{CB\text{-}P}$ and t_b correspond to fault wave arrival, expected DCCB opening and activation of backup protection instants, respectively. The dashed line describes the trajectory of the voltage and current when the DCCB operates. The time interval $[t_0,t_C]$ in Figs. 2 and 3 represents the time frame 'T', which encompasses the interval between the instant of the fault wave arrival at R_{A1} and the moment when the samples from relay R_{B1} or R_{C1} enter Zone 1.

The border line of the zones (threshold line) can be derived by collecting the data of Relays R_{A1}, R_{B1} and R_{C1} in Fig. 1. The collected data should include the voltages and currents at these terminals within a constant time frame for low and high impedance faults in the first zone of R_{A1}. By utilizing Linear Discriminant Analysis (LDA), the threshold line can be found [9].

The data are classified into two sets. The first set consists of the samples of the current and voltage measurements at primary relay of the line (R_{A1}), which is associated with Zone 1, and the second set consists of the samples of the current and voltage measurements at the relay R_{B1} and R_{C1}, which is associated with Zone 2. Identifying the time frame is important to determine the required time for the breaker to operate.

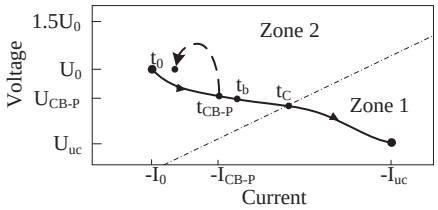

Fig. 2 Loci of voltage and current measurements as function of time as perceived by a relay in zone 2, when (a) the primary protection breaker is triggered at $t_{CB\text{-}P}$ and (b) fault remains uncleared [10].

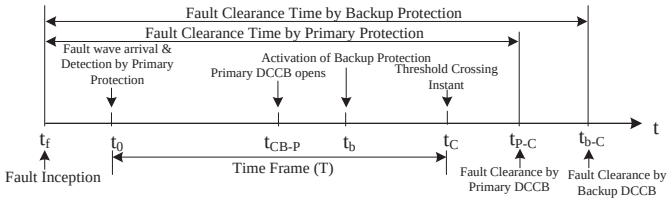

Fig. 3 The continua of the proposed primary and backup protection algorithm.

The principle of operation of the proposed algorithm for R_{A1} is illustrated in Fig. 4. It starts its operation by taking a measurement sample which consists of voltage and current at the terminal of the line. The current is substituted in the threshold line equation ($u_{th}=a\times i_{A1}+b$, where i_{A1} is the current measurement at R_{A1}) to find the threshold voltage u_{th}. The current derivative is calculated using the present and previous current values. The algorithm compares the voltage measurement u_{A1} with the calculated threshold value u_{th} and check the sign of di_{A1}/dt. According to (2) the algorithm will decide to provide primary or backup protection.

$$\begin{cases} u_{A1} < u_{th}, and \dfrac{di_{A1}}{dt} > 0 \rightarrow \text{Forward Fault in Zone 1} \\ u_{A1} > u_{th}, and \dfrac{di_{A1}}{dt} < 0 \rightarrow \text{Backward Fault in Zone 2} \end{cases} \quad (2)$$

1) Primary Protection Principle

The part bounded by the red line in Fig. 4, is responsible for the primary protection. The primary protection is activated when a forward fault in Zone 1 is detected. As a consequence, a detection signal $S_{T\text{-}P\text{-}A1}$ changes from 0 to 1. The signal 'S_{UC}' reflects the variation in the voltage when the DCCB operates as described in (3), where t_{A1} is the required time for A_1 to operate.

$$\begin{cases} u_{A1}(t_{A1}) < u_{DC} \rightarrow \text{Fault remains uncleared} \rightarrow S_{UC} = 1 \\ u_{A1}(t_{A1}) > u_{DC} \rightarrow \text{Fault cleared} \rightarrow S_{UC} = 0 \end{cases} \quad (3)$$

Furthermore, $S_{P\text{-}A1}$ is the output of the AND gate which has $S_{T\text{-}P\text{-}A1}$ and S_{UC} as inputs. When the fault is detected in the first zone, $S_{P\text{-}A1}$ will be 1 until the primary DCCB starts to operate then it falls to 0. However, if the DCCB fails to open, $S_{P\text{-}A1}$ will stay 1 to activate the backup protection as described later.

2) Backup Protection Principle

The green line in Fig. 4 bounds the part which performs the backup protection. After the detection of the backward fault in Zone 2 according to (2), R_{A1} receives two signals from the adjacent relays $S_{P\text{-}B1}$ from R_{B1} and $S_{P\text{-}C1}$ from R_{C1}. If one of these signals is 1, a detected backward fault by the primary protection is identified, and a timer is triggered. When the timer exceeds the required time of the primary DCCB to operate, the relay will recheck the signals from the adjacent relays. If both signals are zero, then the fault is cleared by the primary protection and no further action is required. However, if one signal is still 1, then the backup protection of R_{A1} detects a primary DCCB failure. As a result, a tripping signal $S_{T\text{-}b\text{-}A1}$ rises to 1. Moreover, the algorithm will detect a primary relay failure in the backward direction when the voltage u_{A1} drops below a threshold value $u_{th\text{-}b}$ and the absolute value of the current is higher than $i_{th\text{-}b}$. The signal $S_{b\text{-}A1}$ is generated and transmitted to the adjacent relays to trip all the breakers connected to the local bus. The backup threshold values are chosen using the UI trajectory of the backup relay as demonstrated in the next section.

The tripping signal, which is transmitted to the DCCB, is the output of the OR gate as shown in Fig. 4. The inputs of the gate represent the primary and backup tripping signals which are generated from the relay, and the backup protection signals which are received from the adjacent relays.

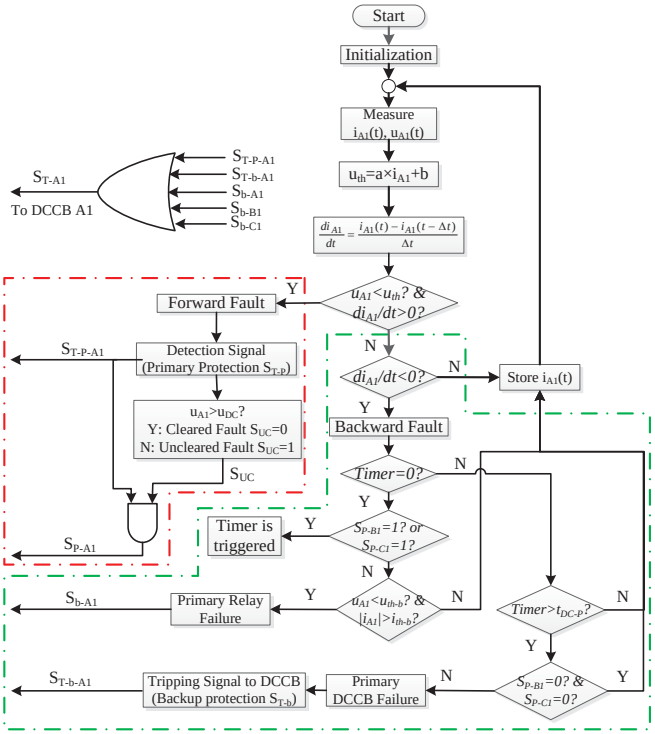

Fig. 4 The flowchart of the proposed protection algorithm for R_{A1}.

Fig. 5 presents the operation of the algorithm as function of time for three cases. The first case is described in Fig. 5(a) when the fault is cleared by the primary protection. Furthermore, it explains the primary DCCB failure case. Fig. 5(b) shows the backup protection when the primary relay fails to detect the fault.

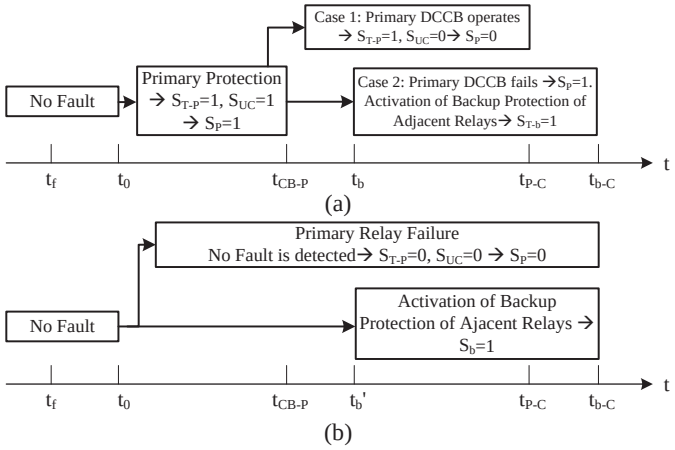

Fig. 5 Primary and backup protection continua, (a) Fault clearance by primary and backup protection in case of DCCB failure, (b) Fault clearance by backup protection in case of primary relay failure.

III. Case Study

The proposed protection algorithm was implemented in a three-terminal symmetrical monopole HVDC test system as shown in Fig. 6 [11]. The test system consists of three terminals which form a delta configuration. Each terminal is connected to a half-bridge modular multilevel converter and two lines per pole. DC breakers are connected to both terminals of each line in series with inductors (100mH) to limit the rate of rise of the fault current. The component models and system parameters are described in [11]. The simulations are performed in PSCAD software to find the threshold lines of the relays and to demonstrate the validity of the protection algorithm.

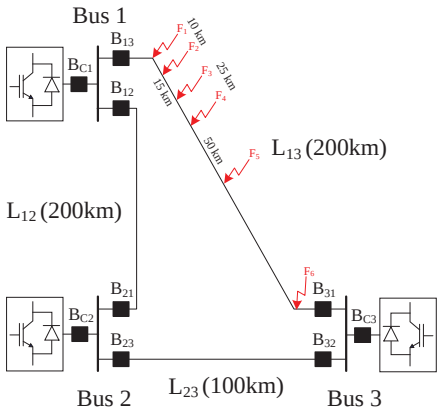

Fig. 6 Three-Terminal HVDC grid test system.

A. Threshold determination of protection zones

To obtain the threshold line equation used by the relay, low impedance and high impedance (10 Ω) faults at different locations on line L_{13} are applied as shown in Fig. 6. Two types of fault simulations are shown, presenting faults at various locations on the line to derive a common threshold line for all

possible scenarios. The distance between faults increases by moving away from B_{13}, since faults located at higher distance from the terminal, generate more attenuated travelling waves. The voltage and current measurements from R_{12} and R_{13} are collected with a sampling frequency of 10kHz. Fig. 7 demonstrates the loci of the voltage and current measurements of the previously mentioned relays for different time frames 'T' (T: is a time delay from t_0, where t_0 is the required time for the voltage wave to arrive at the terminal after the fault inception instant → t_0=0 for F_1; however, t_0=1ms for F_6). The projections of the samples of R_{12} onto UI-plane represent the voltage and the negative value of current, as explained previously.

Linear discriminant analysis was applied to the two samples sets for a time frame T=3ms (Fig. 7(c)) in order to find the threshold line equation as shown in Fig. 8. Equation (4) represents the threshold line formula, where $u_{th}(t)$ represents the threshold voltage in kV and $i_R(t)$ is the current measurement at the relay in kA. The red samples which are close to the blue ones can be ignored, since they represent the samples from the consecutive reflected waves for the close faults seen by R_{13}. As a demonstrative example, the first and second samples of F_2 are shown in Fig. 8. Although the second sample is located in Zone 2, the protection algorithm detects the fault from the first incident wave (First sample), since this sample is located in Zone 1.

$$u_{th}(t)=44.4\times i_R(t)+28.32 \quad (4)$$

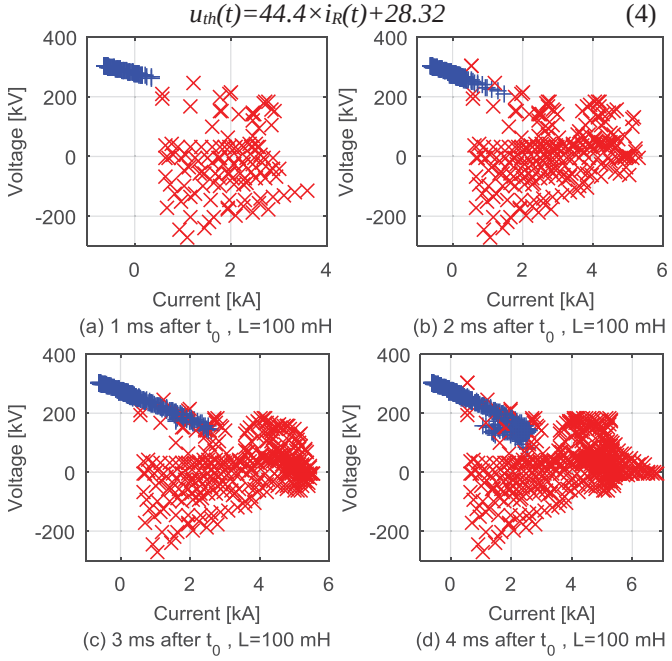

Fig. 7 Loci of voltage and current for faults in L_{13}.
+: $[u^k_{R12}, -i^k_{R12}]$, ×: $[u^k_{R13}, i^k_{R13}]$, k: k^{th} sample

Relay R_{13} detects the forward fault F_1 in its protection zone directly after the inception of the fault, since its samples are located in Zone 1. However, R_{13} senses the forward fault F_6 1ms after the fault occurrence due to the limited speed of the travelling waves. As a consequence, the primary protection and tripping signals of DC breaker B_{13} will be activated within 1ms after the fault inception depending on the fault location (~0ms for F_1 and ~1ms for F_6). On the contrary, R_{12} detects a backward fault and the samples are associated with Zone 2 during the first 3ms for F_1 and 4ms for F_6; however, the samples will be in Zone 1 afterwards (Fig. 7 (d)).

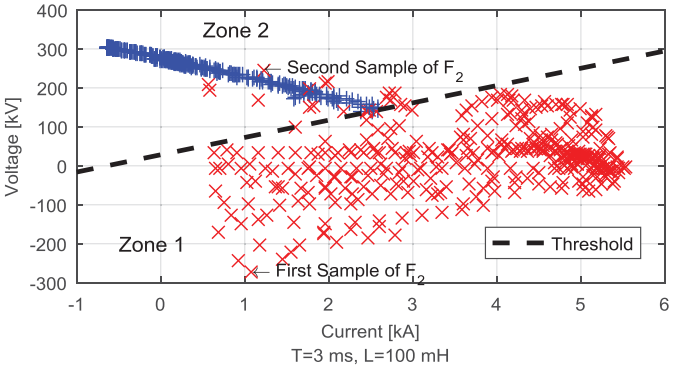

Fig. 8 Threshold line which separates 'Zone 1' and 'Zone 2'.

An adequate time should be kept for DCCB of the backup protection to operate in case of primary protection failure, in order to avoid undesired tripping of remote DCCBs. Hence, T is divided into primary and backup intervals with a short delay. The primary DCCB operates within 1.5ms, and a delay time of 0.5ms is set between the primary and the backup protection in case of primary DCCB failure. Consequently, the backup DCCB operates after 3.5ms. The threshold values of the backup protection for the primary relay failure condition are set to 1.45kA and 215kV. The measurements of R_{12} will cross these thresholds after 2ms from t_0. Fig. 9 shows the current and voltage measurements at R_{12} when a solid fault at t=710ms in the midpoint of L_{13} is applied. The current and voltage of R_{12} crosses the backup threshold values (1.45kA and 215kV) at t= 712.6 (2ms after t_0=710.6ms). Thus, the backup DCCBs will open after 3.5ms as well.

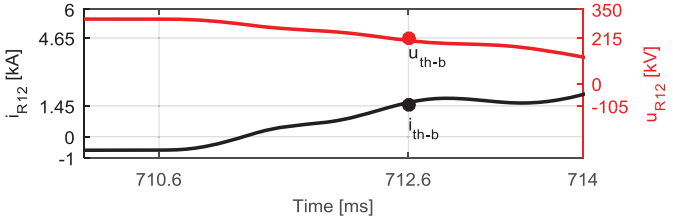

Fig. 9 Current and voltage waveforms at R_{12} for a solid fault at F_5.

Fig. 10 demonstrates the current through B_{13} and the output control signals of R_{12} and R_{13} of the previous mentioned fault for 3 scenarios, where: (a) B_{13} clears the fault, (b) B_{13} fails to clear the fault, hence the backup protection clears the fault by tripping B_{12} & B_{C1} and (c) R_{13} fails to detect the fault, thus the backup protection clears the fault by tripping B_{12}, B_{13} & B_{C1}.

The primary protection detects the fault immediately after the fault wave arrives at the terminal at t=710.6ms and the control signals $S_{T\text{-}P\text{-}R13}$ & $S_{P\text{-}R13}$ become 1 as shown in Fig. 10(a). After 1.5ms from the fault detection, which is the required time for the DCCB to operate, $S_{P\text{-}R13}$ drops to zero as an indication that the primary protection has dealt with the fault due to the rise of the voltage at B_{13} above the threshold value (320kV) as presented in Fig. 11. As a result, the backup protection is activated.

Although the fault is detected by the primary relay in Fig. 10(b), B_{13} fails to interrupt the current. Consequently, the

backup protection is activated by changing $S_{T\text{-}b\text{-}R12}$ to 1 after 2ms from the detection of the fault by R_{13}. Therefore, B_{12} and B_{C1} starts to operate after 3.5ms from the instant of fault wave arrival. However, if R_{13} fails to detect the fault as illustrated in Fig. 10(c), the fault detection by R_{12} will be delayed by 2ms, and the interruption starts 1.5ms after the detection (3.5ms after the incident wave reaches R_{13}). In all scenarios, the fault will be cleared within the first 3.5ms.

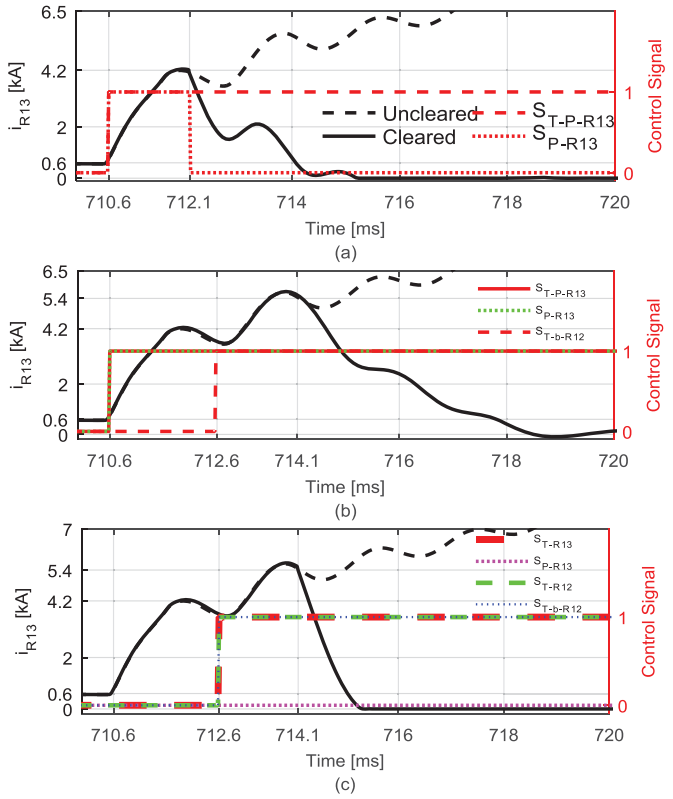

Fig. 10 The current through B_{13} for uncleared and cleared low impedance faults at the mid-point of L_{13}. (a) Cleared fault by primary protection, (b) cleared fault by backup protection with B_{13} failure, (c) cleared fault by backup protection with R_{13} failure.

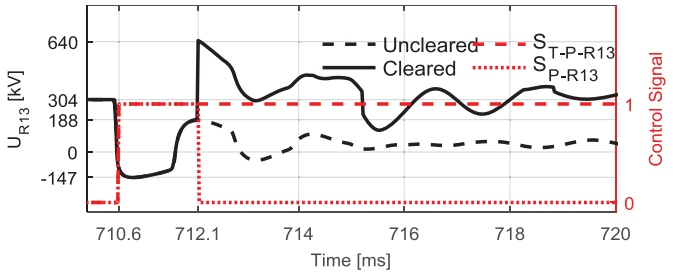

Fig. 11 The voltage at R_{13} for uncleared and cleared fault by B_{13}.

B. *Increasing the time frame 'T'*

The time frame is important to identify the required time for the DCCB to operate. The required time frame of T=3 ms sets the requirements for the protective equipment, most importantly the DC breaker. This time frame fits the currently announced, solid-state and hybrid DCCBs to clear the faults; however, slower devices are not applicable (e.g. current mechanical DCCBs have an optimistic opening time of the contacts of 4 ms [12]). The time frame can be extended by increasing the line inductors or by applying various methods of statistical classification (non-linear discriminant analysis or k nearest neighbor algorithm).

1) Effect of varying the line inductance

The line inductance retards the penetration of the fault to other parts of the grid as it limits the rate of change of the current. The time frame is proportional to the value of the line inductance as illustrated in Fig. 12. The time frame is extended from 1.8ms for L=50mH to 6ms for L=200mH. Furthermore, the threshold line and the protection zones are affected by the inductor value. Equations (5) and (6) represent the threshold lines for 50 mH and 200 mH cases, respectively.

$$u_{th}(t)=42.3\times i_R(t)+31.5 \quad (5)$$

$$u_{th}(t)=50\times i_R(t)+23 \quad (6)$$

2) Extending time frame by statistical classification

As shown previously, although the data of the protection zones can be easily discriminated by a simple line using LDA during the first few milliseconds of the fault (the first 3ms in case of L=100mH), this time frame is not sufficient for slow DCCB to operate. Therefore, the time frame can be extended with constant line inductor by dividing the UI-plane to various areas, where LDA can be applied to each area to derive a piece-wise threshold line which separates the protection zones. In Fig. 13, the UI-plane is split into two areas; the first area is bounded by the red square, and the green square borders the second area. As a result of using LDA for both areas with their associated samples, two lines were derived. The black dashed line represents the threshold line for the relay with time frame T=4ms, and the relay can discriminate the zones according to (7).

$$\begin{aligned} u_{th}(t)&=25\times i_R(t)+17.8 && \text{for } i_R(t) < 2.7kA \\ u_{th}(t)&=96\times i_R(t)-174.4 && \text{for } i_R(t) \geq 2.7kA \end{aligned} \quad (7)$$

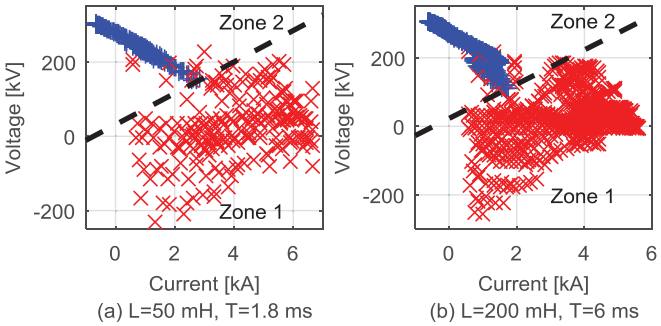

Fig. 12 The effect of changing L on time frame and threshold line.

Moreover, quadratic discriminant analysis (QDA) can be used as shown in Fig. 14 to derive the quadratic function described by (8) with T=4.4ms. However, the samples during fault clearance should be included in the data set to avoid unwanted tripping of adjacent or remote DCCBs during this period.

$$i_R(6.8\times i_R-33.9)+u_{th}(0.0003\times u_{th}-0.7)+0.14\times i_R\times u_R+63.2=0 \quad (8)$$

IV. Conclusion

This contribution proposes a data-based algorithm for primary and backup protection for selective HVDC grid protection system and fast DCCBs based on the local current and voltage measurements. The algorithm projects the measurements onto UI-plane and compares the resulted point to

a predefined threshold in order to extract the classification of the sample, and accordingly it gives the appropriate decision to the relay. The operational principle of the algorithm is divided into primary protection, which detects 'Zone 1' faults at the instant of the incident wave arrival at the terminal, and backup protection, which operates within 0.5ms after the failure of the primary protection.

The algorithm depends mainly on the behavior of the fault propagation in the grid. Therefore, different values of line inductor are studied to investigate the impact of changing the line inductor on the performance of the algorithm. The threshold line and the time frame of the algorithm are sensitive to any change in L. As L increases, the time frame and the slope of the threshold line increase, which gives the opportunity to use DCCB with longer operating times. On the other hand, increasing the line inductor will increase the time constant of the system and increase the requirements of the DCCB. Therefore, two methods of statistical classification using LDA and QDA are discussed with constant L in order to increase the time frame to be longer than the operating time of the slow DCCB.

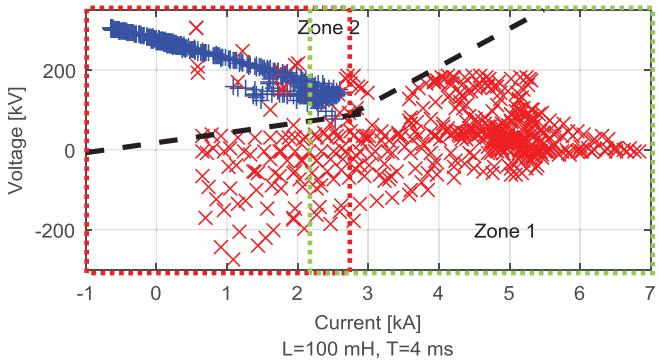

Fig. 13 Threshold after extending T by dividing UI-plane into two areas.

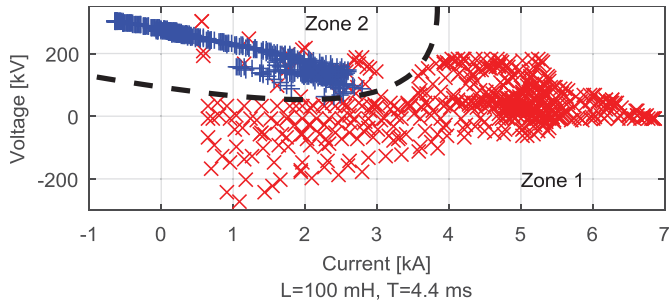

Fig. 14 Threshold line after extending the time frame using QDA.

V. Acknowledgments

This paper presents results from a research project financed and supported by Mitsubishi Electric Corporation. The authors gratefully acknowledge this support.

References

[1] D. Van Hertem and M. Ghandhari, "Multi-terminal VSC HVDC for the European supergrid: Obstacles," *Renew. Sustain. Energy Rev.* vol. 14, no. 9, pp. 3156-3163, 2010.

[2] V. Akhmatov, M. Callavik, C. Franck, S. Rye, T. Ahndorf, M. Bucher, H. Muller, F. Schettler, and R. Wiget, "Technical guidelines and prestandardization. work for first HVDC grids," *IEEE Trans. Power Del.*, vol. 9, no. 1, pp. 327–335, Feb. 2013.

[3] D. Van Hertem, M. Ghandhari, J. Curis, O. Despouys, and M. Andrée, " Protection requirements for a multi-terminal meshed DC grid," in *Cigrè International Symposium The Electric Power System of the Future Integrating supergrids and microgrids*, Bologna, 2011.

[4] P. Anderson, "Power System Protection. Hoboken," NJ, USA: Wiley, 1998.

[5] W. Leterme, J. Beerten, and D. Van Hertem, "Non-unit protection of HVDC grids with inductive dc cable termination," *IEEE Trans. Power Del.*, vol. 31, no. 2, pp. 820-828, 2016.

[6] L. Tang, "Control and protection of multi-terminal dc transmission systems based on voltage-source converters," Ph.D. dissertation, McGill University, Montreal, QC, Canada, 2003.

[7] J. Yang, J. Fletcher, and J. O'Reilly, "Multiterminal dc wind farm collection grid internal fault analysis and protection design," *IEEE Trans. Power Del.*, vol. 25, no. 4, pp. 2308–2318, Oct. 2010.

[8] K. De Kerf, K. Srivastava, M. Reza, D. Bekaert, S. Cole, D. Van Hertem, and R. Belmans, "Wavelet-based protection strategy for dc faults in multi-terminal VSC HVDC systems," *IET Gen., Transm. Distrib*., vol. 5, no. 4, pp. 496–503, Apr. 2011.

[9] R. A. Fisher, "The use of multiple measurements in taxonomic problems", *Ann.Eugen.* 7 (2) (1936) 179–188.

[10] W. Leterme, S. Pirooz Azad, D. Van Hertem, "Fast Breaker Failure Backup Protection for HVDC Grids", in *Proc. IPST 2015 IPST*, Cavtat, Croatia, 15-18 Jun. 2015. , pp. 1-6

[11] W. Leterme, N. Ahmed, L. Ängquist, J. Beerten, D. Van Hertem, S. Norrga, "A newHVDC grid test system for HVDC grid dynamics and protection studies in EMTP," in *Proc. IET ACDC*, Birmingham, UK, 2015.

[12] M. K. Bucher, and C. M. Franck, "Fault Current Interruption in Multiterminal HVDC Networks," *IEEE Trans. Power Del.*, vol. 31, no. 1, pp. 87-95, 2016.

Mudar Abedrabbo received the B.Sc. degree in electrical engineering from Birzeit University, Birzeit, Palestine, in 2009 and the M.Sc. degree in electrical power engineering from RWTH Aachen University, Aachen, Germany in December 2014. He is currently a PhD student at University of Leuven, Leuven, Belgium. His main research interests are protection of HVDC Transmission, Modular Multi-Level Converters and renewable energy integration.

Dirk Van Hertem (S'02–SM'09) received the M.Eng. degree in electromechanical engineering from the KHK, Geel, Belgium, in 2001 and the M.Sc. degree in electrical engineering and Ph.D. degree in electrical engineering from the KU Leuven, Leuven, Belgium, in 2003 and 2009, respectively. In 2010, he was a member of EPS group at the Royal Institute of Technology, Stockholm, Sweden, where he was the Program Manager for controllable power systems for the EKC2 Competence Center. Since 2011, he has been back with the University of Leuven, where he is an Assistant Professor in the Electa group. His special fields of interest are power system operation and control in systems with flexible ac transmission systems and high-voltage direct current and building the transmission system of the future, including offshore grids and the supergrid concept. Dr. Van Hertem is an active member of the IEEE Power and Energy Society, IEEE Industry Applications Society, and CIGRÉ.

Contact Information

Mudar Abedrabbo is with Electa/Energyville, ESAT, KU Leuven University, Kasteelpark Arenberg 10 (PB2445), 3000 Leuven, Belgium (phone number: +3216323976, fax number: +3216321985, e-mail: mudar.abedrabbo@kuleuven.be).